Neuron, Vol. 28, 955–966, December, 2000, Copyright ©2000 by Cell Press

Developmental Remodeling of the Retinogeniculate Synapse

Chinfei Chen* and Wade G. Regehr
Department of Neurobiology
Harvard Medical School
Boston, Massachusetts 02115

Summary

Anatomical rearrangement of retinogeniculate connections contributes to the refinement of synaptic circuits in the developing visual system, but the underlying changes in synaptic function are unclear. Here, we study such changes in mouse brain slices. Each geniculate cell receives a surprisingly large number of retinal inputs (>20) well after eye-specific zones are formed. All but one to three of these inputs are eliminated over a 3-week period spanning eye opening. Remaining inputs are strengthened ~50-fold, in part through an increase in quantal size, but primarily through an increase in the number of release sites. Changes in release probability do not contribute significantly. Thus, a redistribution of release sites from many inputs to few inputs at this late developmental stage contributes to the precise receptive fields of thalamic relay neurons.

Introduction

Synapse elimination and maturation are important developmental processes that contribute to circuit refinement in the nervous system (Brown et al., 1976; Constantine-Paton et al., 1990; Fraser, 1992; Katz and Shatz, 1996; Lichtman, 1977; Lichtman and Colman, 2000; Mariani and Changeux, 1981; Purves and Lichtman, 1980). The retinogeniculate connection is a model system used to study developmental refinement of synaptic circuits in the central nervous system. Anatomical studies demonstrate that significant rearrangement of retinal ganglion cell terminal axons occur after initial connections are formed (Campbell and Shatz, 1992; Mason, 1982; Sretavan and Shatz, 1986; Sur et al., 1984). These changes are thought to contribute to the sharpening of geniculate cell receptive fields, which occurs during a comparable time period (Blakemore and Vital-Durand, 1986; Daniels et al., 1978; Tavazoie and Reid, 2000; Tootle and Friedlander, 1989). Ultimately in adults, geniculate neurons receive sensory inputs from very few retinal ganglion cells and, in some cases, from a single retinal ganglion cell (Hamos et al., 1987).

Although anatomical and in vivo experiments suggest that remodeling occurs at this synapse during development (Katz and Shatz, 1996; Tavazoie and Reid, 2000), the number of retinal ganglion cells initially connected to a given geniculate neuron, and the degree and time course of input elimination are not known. Moreover, the mechanisms underlying the change in strength of the remaining synapses are not completely understood. Both the ability to strengthen these synapses by high frequency stimulation and the increased importance of AMPA receptors compared to NMDA receptors during development suggest that long-term potentiation (LTP) is important (Mooney et al., 1993; Ramoa and McCormick, 1994). However, it is not known if changes in release probability, number of release sites, or quantal size play an important role in the refinement of the retinogeniculate connection.

Here, we examine the changes that occur during visual development at synapses between individual retinal ganglion cells and geniculate neurons. We study the synapses in a mouse brain slice preparation for a number of reasons. First, the mouse brain is compact and a large proportion of the dLGN and its optic tract connections can be preserved in a single tissue section. Second, neurons tend to be small and amenable to voltage clamp studies. Finally, the mouse offers the potential for future genetic approaches.

We find that immediately prior to eye opening each geniculate neuron receives weak synaptic inputs from more than twenty retinal ganglion cells. The mature pattern of innervation, with 1–3 dominant inputs driving each geniculate neuron, is only apparent 2 weeks after eye opening. Thus input elimination is prominent at the retinogeniculate connection, as is the case at the well studied neuromuscular junction (NMJ). Moreover, one, or a small number of remaining inputs strengthen ~50-fold. In contrast to the NMJ, an increase in release probability does not contribute significantly to the strengthening of this central synapse. Instead, synaptic strengthening reflects increases in both AMPA-receptor quantal size and number of release sites. This increase in the quantal size, and the prevalence of "silent synapses" in young animals, suggest that AMPA-receptor insertion is involved.

Results

We studied the retinogeniculate synapses of Black Swiss mice in parasagittal brain slices. This slice orientation contains several millimeters of the optic tract and preserves a high level of connectivity between the retinal ganglion axons and geniculate neurons in the dorsal lateral geniculate (dLGN). The optic tract and projections from the contralateral eye are apparent in the fluorescent image of retinogeniculate fibers labeled with DiI (Figure 1A).

Monosynaptic retinogeniculate synaptic currents are studied as indicated in the schematic (Figure 1A, right). A bipolar electrode is placed 0.6 to 1.2 mm away from the recording electrode and used to activate optic tract fibers without contamination from corticothalamo-fibers and brainstem inputs. Synaptic currents are measured with whole cell voltage clamp from visually selected geniculate neurons. By cutting the connections between the cortex and subcortical structures and recording in

*To whom correspondence should be addressed at The Children's Hospital, Division of Neuroscience, 300 Longwood Avenue, Boston, Massachusetts 02115 (e-mail: chinfei_chen@hms.harvard.edu).

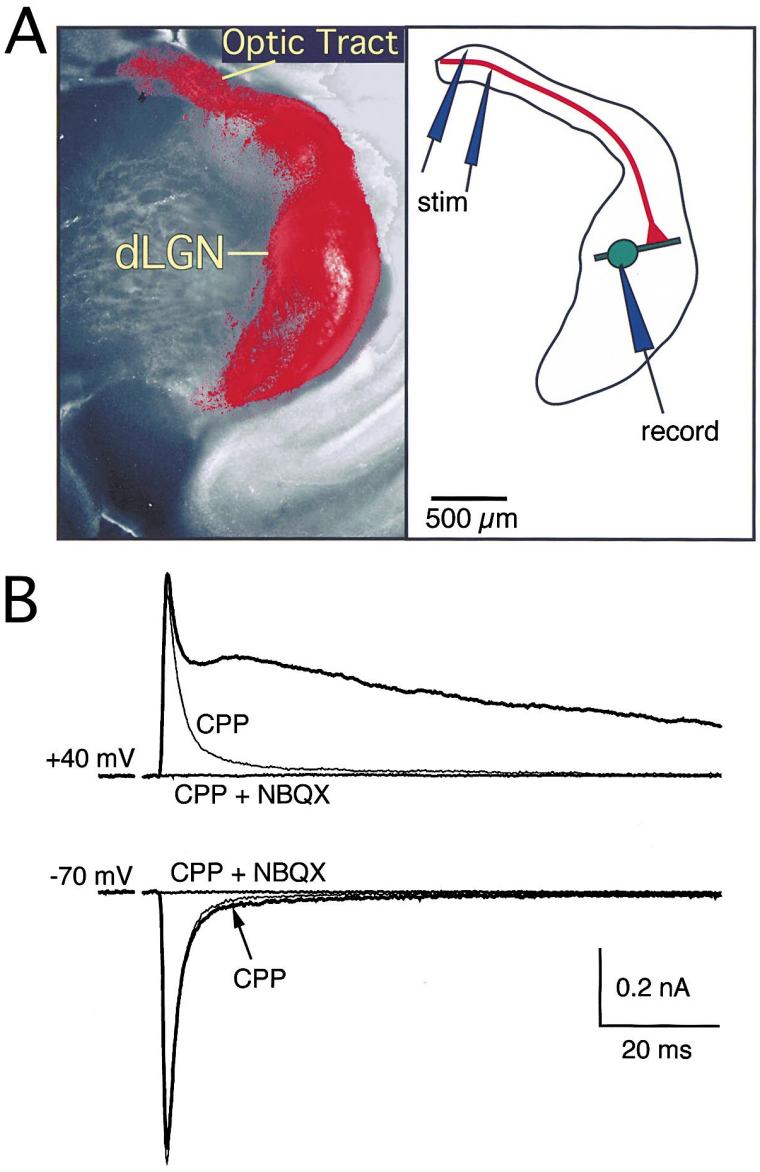

Figure 1. A Slice Preparation of the Mouse Dorsal Lateral Geniculate

(A) Image of the brain slice preparation. DiI was injected into the contralateral retina two days prior to cutting slices. The labeled retinogeniculate fibers (red) are shown as they radiate from the optic tract and synapse onto neurons in the dLGN. For orientation, the hippocampus is located just to the lower right of the dLGN. Schematic of the recording configuration is shown on the right. The retinogeniculate fiber is shown in red, and the geniculate neuron in green.

(B) Pharmacologic sensitivity of the excitatory synapse. Synaptic currents elicited at holding potentials of −70 mV and +40 mV before (bold lines) and after addition of a competitive NMDAR antagonist, CPP only (5 μM, thin lines), and after further addition of NBQX, a non-NMDAR antagonist (5 μM CPP + 5 μM NBQX,thin lines, flat trace). Stimulus artifacts are blanked for clarity. Traces are the average of five trials.

the presence of a $GABA_A$-receptor antagonist, bicuculline, there are no recurrent excitatory or inhibitory circuits activated by stimulation of the optic tract.

We found that retinogeniculate EPSCs are mediated by both NMDA receptors (NMDAR) and AMPA receptors (AMPAR) (Figure 1B). The AMPAR component was identified based on its insensitivity to the NMDAR antagonist CPP, and its complete inhibition by either the non-NMDAR antagonist NBQX (5 μM, n = 5), or GYKI 53655 (30 μM, n = 3, data not shown), the selective AMPAR antagonist that does not inhibit kainate receptors. The NMDAR component was identified by its sensitivity to CPP (5–20 μM, n = 5), its slow time course, and its voltage dependence.

Both NMDAR and AMPAR components can be studied by measuring EPSCs alternately at −70 mV and +40 mV. At −70 mV the peak inward current provides a measure of the AMPAR component of the EPSC. There is very little contamination by NMDAR EPSCs at this holding potential due to Mg^{2+} block. At +40 mV both AMPAR and NMDAR components are apparent. Because the AMPAR evoked EPSC decays with a time constant of 2–3 ms at +40 mV, the peak synaptic current more than 10 ms after the onset of the EPSC provides a good measure of the NMDAR component.

Population Responses Reveal Developmental Changes in Synaptic Currents

We studied the properties of synaptic currents over a 3-week period spanning the time of eye opening, which typically occurs at p14 in these mice. A large stimulus pulse was used to excite many retinogeniculate fibers and the resulting EPSCs were monitored at +40 mV and −70 mV. As shown by the EPSCs obtained from 3 representative experiments (Figure 2), there is a clear developmental trend. Before eye opening (p10–14) the NMDAR component predominates, while immediately after eye opening (p16–22) the AMPAR component in-

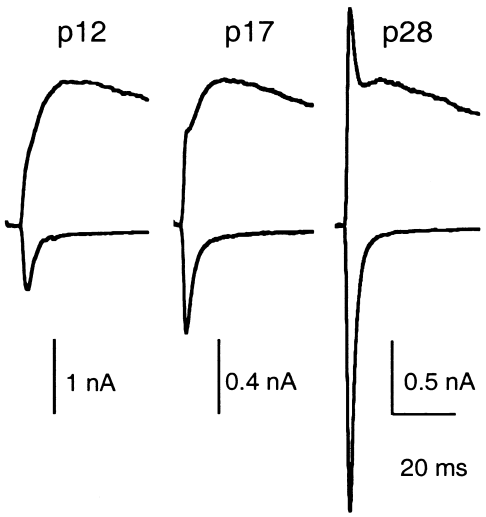

Figure 2. Characteristics of the Mouse Retinogeniculate Synapse

Comparison of the excitatory synaptic currents at different ages. EPSCs were recorded at a holding potential of +40 mV (outward current), and −70 mV (inward current). Currents are normalized to the peak NMDAR current in order to compare the relative amplitude of the AMPAR current. Traces are averages of 5–10 trials.

creases. By young adulthood (p23–31), the AMPAR component is prominent. The average AMPAR/NMDAR peak current ratio increased from 0.5 before eye opening to 2.4 in young adults (Table 1). This large change in the AMPAR/NMDAR current ratio suggests that synaptic scaling alone cannot account for refinement at this synapse (Watt et al., 2000). We also find a developmental trend in the kinetics of the NMDAR current. The decay of the NMDAR current accelerates about 1.5-fold over a three week period (Table 1).

Developmental Refinement in the Pattern of Innervation

Changes in the NMDAR/AMPAR ratio and NMDAR kinetics indicate that significant synaptic refinement is occurring at retinogeniculate synapses after eye opening. Yet the mechanisms responsible for the changes in synaptic properties are not known. One possibility is that they reflect the insertion of AMPAR, as has been described at hippocampal synapses during the induction of LTP (Isaac et al., 1995; Luscher et al., 1999; Malenka and Nicoll, 1999; Shi et al., 1999). An alternative explanation is that the NMDAR component is reduced (Ramoa and McCormick, 1994). It is not possible, however, to distinguish between these hypotheses by examining the population response of many activated retinal ganglion cell fibers, because the number of axons stimulated is different in each experiment. One way to provide insight into the mechanisms responsible for synaptic refinement is to examine the properties of individual fibers.

As a step toward characterizing the behavior of individual retinothalamic fibers, we systematically stimulated the optic tract over a range of stimulus intensities (0–40 μA). We hypothesized that more retinogeniculate fibers would be recruited as the stimulus intensity increased. Before eye opening, there is an incremental increase in the synaptic current in response to stronger stimulus intensities (Figure 3A). In this example the peak EPSC evoked by 40 μA stimulation is over 400 pA for the NMDAR and over 150 pA for the AMPAR. The largest incremental increase evoked by elevating stimulus intensities is about 100 pA for the NMDAR and less than 20 pA for the AMPAR. These findings suggest that this geniculate neuron is innervated by many fibers, and that each fiber contributes a relatively small synaptic input. Soon after eye opening (p17; figure 3B), however, the incremental increases in synaptic current evoked by stronger stimuli acquire a discrete, step-like character. When compared to the younger animals, there are fewer "steps" in synaptic current amplitude, and some increments in the current are as large as 400 pA for the NMDAR component and 500 pA for the AMPAR component. Thus, this neuron is innervated by multiple retinal ganglion cells, some weakly connected and others quite powerfully connected. In young adults (p28), the trend continues (Figure 3C), and only one synaptic contact is apparent in this example. It has an NMDAR component

Table 1. Summary of the Properties of the Retinogeniculate Synapse for Different Postnatal Ages

Synaptic Property	p10–14	p16–22	p23–31
Amplitude at 40 μA stimulus (pA)			
AMPAR#	−230 ± 60, n = 24	−570 ± 100, n = 27	−1220 ± 150, n = 18
NMDAR	460 ± 90, n = 31	540 ± 120, n = 27	520 ± 80, n = 17
NMDAR decay τ (ms)†	150 ± 13, n = 24	120 ± 12, n = 19	90 ± 8, n = 11
AMPA/NMDA peak current ratio*#	0.5 ± 0.1, n = 30	1.3 ± 0.2, n = 27	2.4 ± 0.4, n = 21
Amplitude single fiber input (pA)			
AMPAR#	−10 ± 4, n = 37	−270 ± 60, n = 47	−750 ± 140, n = 28
NMDAR#	26 ± 6, n = 38	160 ± 40, n = 45	370 ± 70, n = 26
Number of "silent" fibers	8/37	2/47	0/28
Paired-pulse ratio	0.73 ± 0.03, n = 5	0.67 ± 0.06, n = 3	0.62 ± 0.01, n = 4
AMPA mEPSC amplitude (pA)†	−6.6 ± 0.2, n = 5	−8.6 ± 1.5, n = 5	−12.5 ± 1.2, n = 4
AMPAR decay τ (ms) from mEPSC	2.2 ± 0.3, n = 5	2.0 ± 0.3, n = 5	1.6 ± 0.1, n = 4

* calculated from each individual experiment

The mean ± SEM for each synaptic property are shown. Statistical analysis of the difference between the means for each property was calculated using the two sample t test, and the significant levels are indicated by the following symbols: # All differences between the groups p10-14 versus p16-22, p16-22 versus p23-31, and p10-14 versus p23-31 are significant to $p \leq 0.01$; † Difference between the p10-14 versus p23-31 groups is significant to $p \leq 0.02$. The means of all age groups for the NMDAR amplitude elicited at 40 μA stimulus, as well as of the AMPA mEPSC decay τ were not significantly different. The difference in the means of the p10-14 versus p23-31 groups for paired pulse ratio is significant to $p \leq 0.03$.

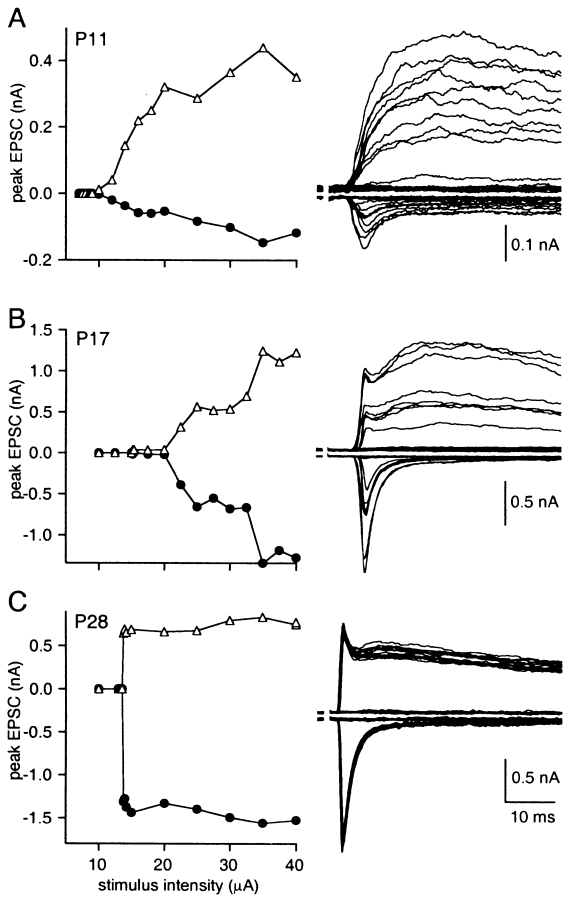

Figure 3. Fewer Retinogeniculate Fibers Are Recruited after Eye Opening

Representative responses to incremental increase in stimulus intensities (up to 40 μA) from animals of different ages. (Left panels) Plots of the peak amplitudes of the AMPAR (black circles) and NMDAR (triangles) components of the synaptic current elicited as a function of stimulus intensity. (Right panels) Superposition of the synaptic currents elicited over the range of stimulus intensities while alternating between holding potentials of +40 mV (outward currents) and −70 mV (inward currents).

of over 500 pA and an AMPAR component of about 1.5 nA. In general, we found that increasing the stimulus intensity over 40 μA (up to 100–600 μA) did not evoke significantly larger synaptic currents.

We observed the same qualitative behavior for synaptic inputs in a number of animals ranging from prior to eye opening (n = 9), to immediately after eye opening (n = 12), to young adults (n = 9). These results demonstrate remodeling of the retinogeniculate connection during a three-week period spanning the time of eye opening. Before eye opening, a geniculate cell receives weak synaptic contacts from many retinal ganglion cells. In young adults, although a few weak inputs remain, the bulk of synaptic drive is provided by one or two very powerful synaptic inputs.

Developmental Changes in Single Fiber Inputs

Despite the clear qualitative developmental trend in the pruning of multiple inputs revealed by varying the stimulus intensity, this method is poorly suited for quantification of the size and number of retinal inputs. Fibers are recruited over a wide range of stimulus intensities, making it impractical to examine synaptic inputs with a sufficiently fine range of stimulus amplitudes. Moreover, because of trial-to-trial stochastic variation only the largest inputs would be identified and small inputs would not be detected. Thus, we used another method to estimate the number of fibers innervating a geniculate cell and to quantify the distribution of their synaptic strengths.

We measured the synaptic properties of individual fibers to obtain more quantitative information on their properties (Figure 4A1). After obtaining a recording from a geniculate cell, stimulus electrodes are positioned in the optic tract so that a synaptic input is activated. The stimulus intensity is then lowered until there is no synaptic response, and then incrementally increased until optic nerve stimulation results in a synaptic response. Amplitudes of the AMPAR (circles) and NMDAR (triangles) currents are plotted as a function of stimulus intensities (Figure 4A2). The sharp transition from failures to a reliable synaptic current is consistent with the activation of a single retinogeniculate fiber. Moreover, further increases in the stimulus intensity over the range shown give rise to the same size synaptic current.

Detection of single fiber inputs was also possible for much smaller synaptic inputs (Figure 4B). For these inputs, it was helpful to use multiple trials at each stimulus intensity. Individual synaptic responses elicited by subthreshold (Figure 4B1) and suprathreshold (Figure 4B2) intensities are shown. Average EPSCs shown below in bold traces and at an expanded scale (Figure 4B3), display the kinetic properties of AMPAR and NMDAR currents. Peak currents of individual trials are plotted as a function of the stimulus intensities (white symbols) to illustrate the threshold response for this small input (Figure 4B4). Average peak AMPAR and NMDAR currents for each intensity are superimposed as well (black symbols). The low frequency of failures seen in consecutive stimulation, even for small inputs, is consistent with a high probability of release.

Some inputs are apparent only when the geniculate cell is held at a depolarized potential (Figure 4C). The average of 10 consecutive trials, alternating between the two holding potentials (Figure 4C1) reveal the absence of a inward current at −70 mV. Individual traces that contribute to these average currents (Figure 4C2) show a reproducible failure when testing for the AMPAR component of the synaptic current. This input must consist of one or more release sites with postsynaptic densities containing only NMDAR and not AMPAR. It is "silent" at −70 mV because of the voltage dependence of NMDAR.

Single fiber responses reveal major developmental changes in the properties of single inputs. Representative examples of single fiber synaptic response from mice of different ages are plotted on the same scale for comparison to illustrate this trend (Figure 5A). Both the NMDAR and AMPAR components of the synaptic response become much larger in young adults.

The same trend is apparent in the summary of single fiber responses from many dLGN cells (Figure 5B, C). Amplitude histograms of the NMDAR and AMPAR responses are shown for the three age groups. In young animals (p10–14), average single fiber inputs are less than 30 pA (Table 1). A fraction of these single fiber

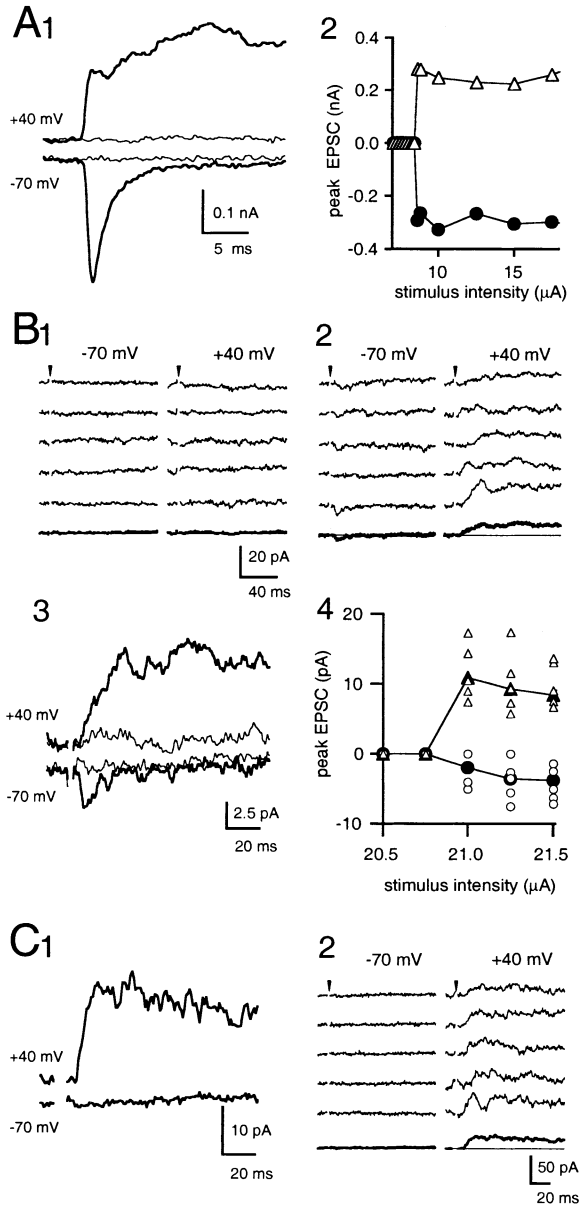

Figure 4. Stimulation of a Single Retinogeniculate Input

(A) Example of the response to stimulating a single retinogeniculate fiber from a p17 mouse. (A_1) An increase in stimulus intensity from 8.4 μA to 8.6 μA results in a sharp transition from a response failure to one that elicited synaptic currents (−291 pA and 283 pA for AMPAR and NMDAR currents, respectively). (A_2) The threshold response is evident when the peak of the AMPAR and NMDAR currents are plotted as a function of stimulus intensities. These findings are consistent with the stimulation of a single fiber.

(B) Individual single fiber responses of a small input from a p11 mouse. Example of ten individual consecutive trials, alternating between −70 mV and +40 mV, elicited at stimulus intensity of 20.75 (B_1) and 21.25 μA (B_2). The average of the 5 trials is shown below each set of traces in bold. (B_3) Superimposed average of the subthreshold and suprathreshold response from above shown at higher magnification. (B_4) The peak responses from 10 consecutive trials are plotted as a function of increasing stimulus intensities (white symbols). Peaks of the average traces at each stimulus intensity were also superimposed (black symbols).

(C) Example of the average response of a silent fiber (C_1). Individual consecutive trials (C_2) for the two holding potentials are shown on the right along with the averages of 5 traces (bold). Evoked recordings are aligned to the time of stimulation (arrowheads).

inputs are silent (8/37 or 22% of total single fibers). The presence of silent synapses has been shown to be important in synaptic plasticity, especially in NMDAR-mediated LTP (Isaac et al., 1997; Malenka and Nicoll, 1999) (see Discussion).

Soon after eye opening (p16–22), the inputs increase in size, ranging from several hundred pA to nA currents. Only 2 of 47 fibers (4%) are silent. The increase in the size of the single fiber inputs continues in young adults (p23–31), as a larger proportion of the AMPAR currents become greater than 1 nA (Table 1). Moreover, no "silent fibers" are observed in these older animals. Each retinogeniculate fiber, however, may contain more than one release site, thus the fraction of "silent synapses" is difficult to estimate in older animals.

Cumulative amplitude histograms of single fiber strength, which are the normalized integrals of the amplitude histograms, are a convenient way of comparing the amplitude distributions at different ages (Figure 5C). For example, comparison of the AMPAR component reveals that about 50% of the inputs are greater than 500 pA in adults, while in young animals, all inputs are smaller than 120 pA. Both the NMDAR and AMPAR components of the single fiber response are larger in older animals. However, the relative increase in the peak AMPAR current over the two week period is greater than that of the peak NMDAR current (about a 60-fold versus 15-fold increase in the average current amplitude of the AMPAR and NMDAR component, respectively).

With the average values we obtained from the size of the total current elicited by a strong stimulus intensity (40 μA), and the amplitudes of single fiber inputs, we can estimate the number of retinal inputs that innervate a geniculate neuron. In young animals before eye opening, this calculation (e.g.: from Table 1, −230 pA/−10 pA for AMPAR or 460 pA/26 pA for NMDAR) yields ~20 inputs. This value represents a lower bound because the slice does not contain all of the retinal fibers, and it may not be possible to activate *all* of the retinal inputs that are present within the slice.

Quantal Size and Probability of Release during Development

Several mechanisms could contribute to the profound increase in the strength of individual synapses connecting retinal ganglion cells to their targets. First, new release sites could be added. The huge increase in the size of the synaptic responses suggests that this is likely. Second, the response to each quanta could become larger, either by increasing the contents of a vesicle or by changing the postsynaptic response to each vesicle. Third, the probability of release could increase, so that in response to fiber activation a larger fraction of the release sites would release a vesicle.

We examined the size of the response to the release of single vesicles by measuring quantal events. Our studies were restricted to quantal events mediated by AMPAR, because the small slow NMDAR currents were extremely difficult to detect. Spontaneous miniature EPSCs could not be used for these studies because geniculate neurons receive glutamatergic inputs from the cortex as well as the retina. We studied evoked quantal events resulting from stimulating the optic tract in the presence of 3 mM $SrCl_2$, 0 mM $CaCl_2$ in the extracellular saline

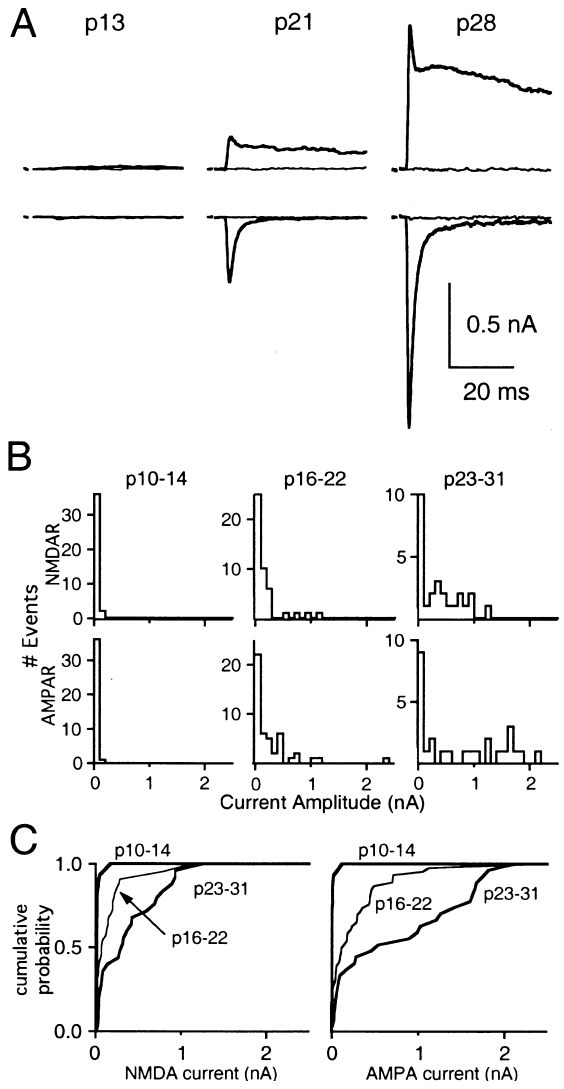

Figure 5. Single Fiber Inputs Become Larger after Eye Opening

(A) Comparison of the single fiber response from three different ages. The response to individual trials are shown. Thin and bold traces indicate the subthreshold and suprathreshold response, respectively, to an incremental increase (0.2 μA–0.5μA) in the stimulus intensity. Outward (top) and inward (bottom) currents were elicited at a holding potentials of +40 and −70 mV, respectively. The amplitudes of the EPSCs (in pA) for NMDAR component are 20, 150, 650 and for the AMPAR component are −13, −407, and −1312 for p13, p21 and p28 animals, respectively. Stimulus artifacts are blanked for clarity.

(B) Amplitude histograms of the NMDAR (top row) and AMPAR (bottom row) component of single fiber inputs over three age groups (p10–14, left column; p16–22, middle column; p23–31, right column).

(C) Cumulative amplitude histograms for the three age groups for the NMDAR (left) and AMPAR (right) components.

solution. Substitution of strontium for calcium is an effective tool used to desynchronize evoked release and thus allow resolution of quantal events (Goda and Stevens, 1994; Miledi, 1966; Xu-Friedman and Regehr, 1999). A similar approach has been used in ferret retinogeniculate synapses, where the amplitude of AMPAR mEPSCs was found to remain constant during ON/OFF sublamination in the dLGN (Hohnke and Sur, 1999).

Here, in a later developmental period spanning eye opening, there is a clear increase in the size of quantal events, as illustrated by the representative recordings of Figure 6. Evoked trials are shown on the left for three representative ages (Figure 6A). Before eye opening the quantal events are so small that they are difficult to detect. After eye opening quantal events become more apparent and, in young adults, many quantal events are larger than 20–30 pA. Amplitude histograms from each example are shown to the right and the average mEPSCs, obtained from several hundred events, are shown in the insets (see Methods). The results from many such experiments are shown in Figure 6B. Normalized cumulative probability histograms from each experiment, obtained from integrating the amplitude histograms, are superimposed for the three age groups. A comparison of the average cumulative amplitude histograms reveals clear differences in these three groups (Figure 6C).

Using our detection criteria, over this developmental period, the quantal size increases from −6.6 to −12.5 pA (Table 1). These values provide an upper bound for the synaptic response to the release of a single vesicle. This is especially true before eye opening, where silent synapses are common and quantal events are sufficiently small that many are lost in the noise. Thus our estimate of a 2-fold increase in the quantal size is a lower bound. Recruitment of new receptors can explain this increase in the AMPAR quantal size. We cannot, however, rule out an additional presynaptic contribution to changes in quantal size, such as an increase in the amount of neurotransmitter associated with a single vesicle.

Another mechanism that could contribute to the developmental increase in the strength of the retinogeniculate synapse is a change in the probability of release. We monitored the AMPAR response to pairs of pulses, which has been widely used to detect changes in the release probability. An increase in the probability of release leads to a decrease in the paired-pulse ratio (ppr), which, for two closely spaced stimuli, is the amplitude of the second EPSC divided by the amplitude of the first EPSC.

In order to monitor presynaptic processes without possible contamination of postsynaptic receptor desensitization, ppr was monitored in the presence of cyclothiazide (CTZ). 20 μM CTZ increased both the AMPAR EPSC amplitude and the ppr at the retinogeniculate synapse (Figure 7A). CTZ has been shown to have presynaptic effects at some CNS synapses (Bellingham and Walmsley, 1999; Diamond and Jahr, 1995). To determine if this is also true at the retinogeniculate synapse, we examined the effects of 20 μM CTZ on the NMDAR response. If CTZ acts presynaptically to alter neurotransmitter release, then the NMDAR response to pairs of pulses would be different in the presence of the drug. Figure 7B demonstrates that 20 μM CTZ does not have presynaptic effects at the retinogeniculate synapse.

The paired-pulse ratio measured in the presence of CTZ was similar before eye opening and in young adults (see Table 1). The extent of paired pulse depression suggests that the probability of release is quite high at all ages tested. Although a precise estimate is difficult, based on a simple depletion model of depression (Ditt-

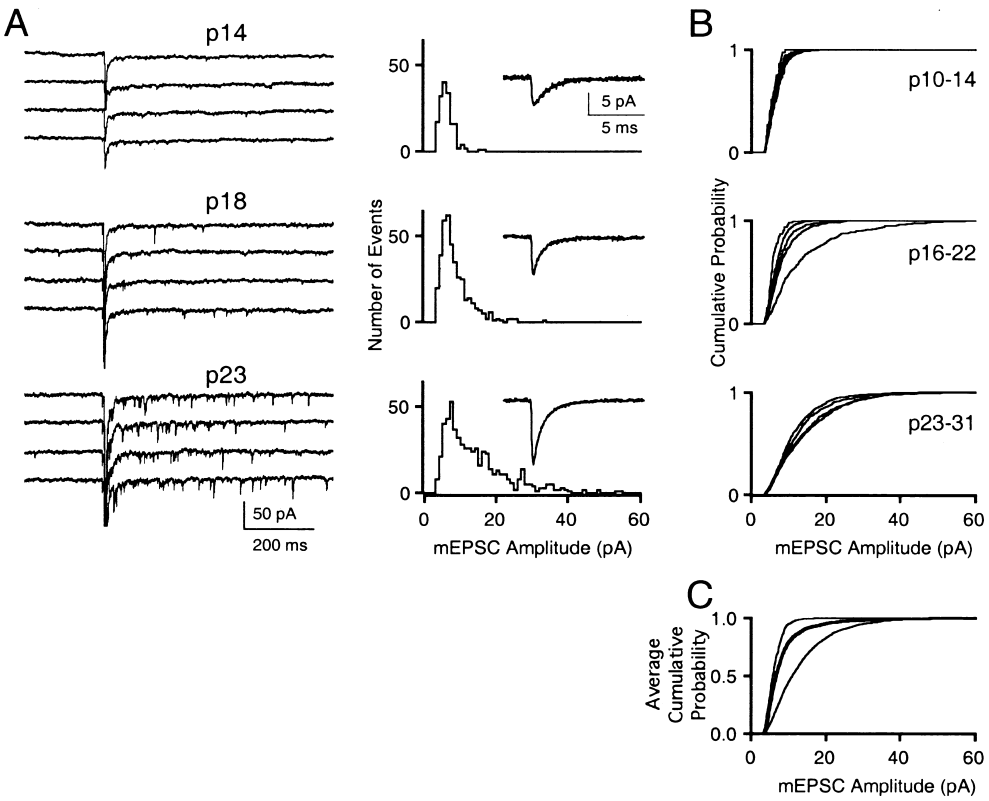

Figure 6. The Size of the Quantal Response at the Retinogeniculate Synapse Increases after Eye Opening

(A) Representative consecutive traces of evoked quantal events, obtained in the presence of 3 $SrCl_2$ and 2 $MgCl_2$, for three different ages. For each example several hundred events were used to obtain the amplitude histogram (right panels) and average mEPSC (right, insets). The three average mEPSCs are plotted on the same scale for comparison (in pA, p14, −6.0; p18, −8.5, p23, −14.7). (B) Normalized cumulative amplitude histograms from all experiments are superimposed for three age groups (p10–14, n = 5; p16–22, n = 5; p23–31, n = 4). The normalized average cumulative amplitude histograms of the three age groups are superimposed below in (C) (p16–22, bold line; p10–14, thin line on left; p23–31, thin line on right). The distributions of these three age groups were all significantly different from each other, ($p << 10^{-4}$, by Kolmogorov-Smirnov test, with the following number of events: p10–14, 990; p16–22, 2519; p23–31, 1737).

man and Regehr, 1998), the extent of ppr is consistent with an initial probability of 0.3 to 0.4 at all ages. These results suggest that, although there may be a small increase in the probability of release at the retinogeniculate synapse, this mechanism does not contribute significantly to changes in synaptic strength over the p10 to p31 range.

Discussion

We find that tremendous synaptic rearrangement occurs at retinogeniculate synapses even after eye-specific zones are formed in the LGN. The loss of some synapses and the strengthening of others ultimately leads to the adult pattern of connections required for precise receptive fields in relay neurons. Synaptic strengthening reflects primarily an increase in the number of release sites, although additional processes are also involved.

The Specificity of Retinogeniculate Input Increases in Adults

A remarkable aspect of our findings is the *degree and timing* of functional synapse elimination and remodeling. Previous work at the retinogeniculate connection has focused on the period when inputs from each eye are segregated into distinct regions within the dLGN. We find that immediately before eye opening each geniculate cell receives weak inputs from at least twenty ganglion cells. It is surprising that a geniculate neuron receives such a large number of inputs at this late developmental stage, long after retinal inputs first invade the LGN and after the formation of eye specific zones, which is largely complete by P8 in mice (Godement et al., 1984). Thus, at the time of eye opening, even though the inputs are in the correct region of the LGN, the synapses do not display the connectivity that is typical of the adult.

At this relatively late phase of development, retinogeniculate synapses are still undergoing significant remodeling. While each geniculate neuron is still innervated by many ganglion cells immediately after eye opening, the strengths of some of these connections increase. Furthermore, the relative contribution of the AMPAR component increases, as does the size of mEPSCs mediated by AMPARs. This functional synaptic remodeling occurs during a time period that corresponds to both a refinement of the receptive field properties of geniculate neurons and to significant changes in retinal ganglion

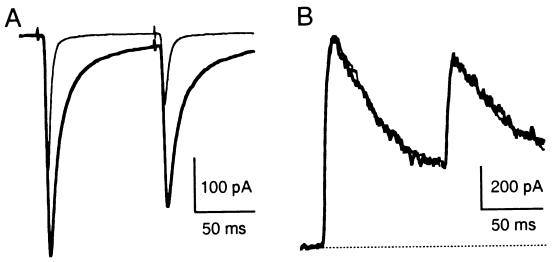

Figure 7. The Effects of Cyclothiazide on the Synaptic Response to Paired-Pulse Stimulation

Example of the synaptic response to a pair of stimuli, in control conditions (thin trace) and after bath application of 20 μM CTZ (bold trace) for the AMPAR (A) and NMDAR (B) currents. In CTZ, the amplitude of the first AMPAR EPSC increased from −521 pA to −850 pA and ppr changed from 0.53 to 0.73. On average, AMPAR ppr is 0.48 ± 0.03 (n = 4) in control conditions and 0.76 ± 0.03 (n = 4) in 20 μM CTZ. AMPAR EPSCs were measured at a holding potential of −40 mV in the presence of 5 μM CPP. In contrast, both the peak current and ppr of NMDAR component, examined at +40 mV in the presence of 10 μM NBQX, were not affected by 20 μM CTZ (NMDAR ppr: control, 0.60 ± 0.08, n = 5; 20 μM CTZ, 0.61 ± 0.07, n = 5). Traces in (A) and (B) are the average of 3 trials and obtained from different experiments.

axon arborization in other mammalian species (Blakemore and Vital-Durand, 1986; Daniels et al., 1978; Sur et al., 1984; Tavazoie and Reid, 2000).

By two weeks after eye opening, the retinogeniculate synapses display their adult pattern of innervation. One to three retinal inputs dominate the postsynaptic cell. Thus the refinement of this CNS synapse involves the redistribution of release sites from many inputs to a few inputs. Based on the average amplitudes of the single fiber input and mEPSC in adults, we estimate that these synaptic responses arise from the release of 50 to 100 vesicles. To estimate the total number of release sites, it is necessary to take into account the probability of release, because not all sites release neurotransmitter in response to each stimulus. Based on a probability of release of 0.4 (see Results) we estimate that in the adult each of the dominant synaptic inputs contribute 125 to 250 release sites, which agrees with anatomical descriptions of the retinothalamic synapses in cats (Hamos et al., 1987). This is also consistent with the receptive field properties of geniculate neurons in adult cats, where the inputs from one or two retinal ganglion cells dominate the receptive field (Cleland et al., 1971; Mastronarde, 1992; Usrey et al., 1999). Although several small inputs are also often observed, most of the small inputs present in young mice, are absent by 4 weeks of age.

Mechanisms Underlying the Increase in Synaptic Strength

We reveal a number of mechanisms that contribute to the marked increase in the synaptic strength seen during development. Several features of the refinement of the retinogeniculate synapse suggest the participation of NMDAR- mediated LTP and the "unsilencing" of synapses through AMPAR insertion (Durand et al., 1996; Golshani and Jones, 1999; Isaac et al., 1995; Isaac et al., 1997; Luscher et al., 1999; Malenka and Nicoll, 1999; Rumpel et al., 1998; Shi et al., 1999; Wu et al., 1996). The increase in the contribution of AMPAR relative to NMDAR to the evoked EPSC, as well as the enhancement in the AMPAR mEPSC size is consistent with the addition of AMPARs. Thus, the observations described in this current study suggest that LTP, which has been proposed to contribute to the early development of the visual cortex (Artola et al., 1990; Kirkwood et al., 1993), the retinotectal connection (Bi and Poo, 1999), and eye-specific lamination prior to eye opening (Mooney et al., 1993), may also be important in synaptic remodeling after eye opening (Constantine-Paton and Cline, 1998).

One striking conclusion from our data is that the increase in the amplitude of the quantal event accounts for only a small fraction of the total increase in the AMPAR component of the single fiber input. Thus, other mechanisms must account for the bulk of the increase in synaptic strength. Since changes in the release probability at this synapse do not contribute significantly to the developmental remodeling that we are studying, we conclude that a substantial increase in the number of release sites accounts for the majority of the increase in synaptic strength. Consistent with this idea is the finding of a 15-fold increase in the NMDAR component of the synaptic current over a 3-week developmental window. The increase in the strength of the NMDAR current cannot be attributed to merely a switch in the receptor subunit composition, which accounts for, at most, a 2-fold difference in conductance (Kutsuwada et al., 1992; Monyer et al., 1992; Ramoa and Prusky, 1997).

Although the mechanisms responsible for the addition of release sites are not yet known, one interesting possibility is that synaptic scaling and redistribution of postsynaptic sites are involved (Davis and Goodman, 1998; O'Brien et al., 1998; Watt et al., 2000). Over the developmental time period that we examined, there does not appear to be a major change in the total NMDAR response to high intensity stimulation (40 μA), suggesting that there is not a prominent change in the total number of NMDARs associated with retinogeniculate synapses. Similarly, our estimates of the total number of release sites associated with retinogeniculate inputs on to each relay cell does not show large changes in this developmental time period. Further experiments are required to determine if these findings reflect a homeostatic mechanism that maintains a constant number of postsynaptic NMDAR and release sites, or if strengthened synapses incorporate the postsynaptic NMDAR from eliminated synapses.

General Implications for Retinogeniculate Development

Numerous features of the retinogeniculate synapse appear to be common to many mammalian species. Retinal inputs from the left and right eye initially overlap in the dLGN and then segregate into eye specific zones in mice, ferrets, and cats (Godement et al., 1984; Linden et al., 1981; Sretavan and Shatz, 1986). After eye opening, the synaptic reorganization that we see in mice is consistent with the postnatal refinement of the LGN receptive field properties in ferrets, cats, and monkeys (Blakemore and Vital-Durand, 1986; Daniels et al., 1978; Tavazoie and Reid, 2000). Furthermore, changes in the kinetic properties of glutamate receptors in ferrets have

been observed during this period at the retinogeniculate synapse (Ramoa and Prusky, 1997). Finally, the mature retinogeniculate connections make glomerular contacts and triadic synaptic arrangements with inhibitory interneurons and geniculate cell dendrites in mice, cats, and monkeys (Hamori et al., 1991; Hamos et al., 1985; Rafols and Valverde, 1973). Thus, the synaptic principles that we have revealed for the mouse visual system are likely to apply to other mammalian species.

Implications of the Developmental Reorganization of the Retinogeniculate Synapse

The multiple retinal inputs that drive a geniculate cell before eye opening may have important consequences for the development of the visual system. The relatively late refinement of retinogeniculate connections corresponds to a period of significant plasticity in the visual cortex. Synaptic enhancement in response to LTP stimulation protocols have been demonstrated in rats up to p30 in age (Kato et al., 1991; Kirkwood et al., 1995). Moreover, ocular dominance plasticity of the primary visual cortex in mice occurs over the 2 week period after eye opening (Fagiolini et al., 1994; Gordon and Stryker, 1996; Hensch et al., 1998), and for weeks to many months in cats (Freeman and Olson, 1982; Shatz and Stryker, 1978; Trachtenberg et al., 2000) and monkey (Blakemore et al., 1978; Hubel et al., 1977; LeVay et al., 1980). A recent study has proposed a Hebbian-based model in which transient convergent synapses between the retina and LGN help refine connections between the LGN and cortex (Tavazoie and Reid, 2000). Consistent with this hypothesis, we show that a surprisingly large number of retinal ganglion cells can influence the firing of each geniculate neuron at the time of eye opening.

Comparison to Developmental Processes at Other Synapses

The retinogeniculate synapse is similar to other synapses in some aspects of its developmental refinement. Comparable developmental changes in NMDAR/AMPAR ratio and NMDAR kinetics have been previously described in the retinogeniculate synapse of ferrets (Ramoa and McCormick, 1994; Ramoa and Prusky, 1997). Moreover, these trends have been noted at other synapses of the visual system, including the visual cortex (Carmignoto and Vicini, 1992), and tectum (Hestrin, 1992; Shi et al., 1997; Wu et al., 1996), although the degree and time course of these changes vary depending on the specific type of connection. Thus the trends that we see in mice may reflect a general developmental theme of many CNS synapses common to several mammalian species (Bellingham et al., 1998; Chuhma and Ohmori, 1998; Constantine-Paton and Cline, 1998; Golshani et al., 1998). These findings demonstrate that synaptic changes occur during a period in which receptive field properties are refined.

In addition to the visual system (Campbell and Shatz, 1992; Katz and Shatz, 1996; Shatz and Kirkwood, 1984), synapse elimination has been observed in other areas of the nervous system (Purves and Lichtman, 1980). The best studied system for synaptic reorganization during development is the neuromuscular junction (NMJ) (Lichtman and Colman, 2000). Here, synapse elimination occurs over the first 2 weeks after birth and is dependent on motor neuron activity (Brown et al., 1976; O'Brien et al., 1978). Reorganization of submandibular ganglion innervation is also associated with a decrease in the number of preganglionic inputs and an increase in the number of synaptic contacts (Lichtman, 1977).

Pruning inputs during development also occurs at several CNS synapses. At the connection between the chick cochlear nerve and nucleus magnocellularis, the average number of inputs decreases from 4 to 2 between embryonic day 13 and 18 (Jackson and Parks, 1982). In the developing rat cerebellum, Purkinje cells are innervated by multiple climbing fibers before postnatal day 8, and by a single climbing fiber by postnatal day 15 (Crepel et al., 1976; Mariani and Changeux, 1981). Such climbing fiber elimination is disrupted in mice lacking mGluR1 and γPKC (Aiba et al., 1994; Kano et al., 1995).

In addition to input elimination, an increase in synaptic strength of remaining inputs is observed at both retinogeniculate synapses and the NMJ (O'Brien et al., 1978). Some of the mechanisms of synaptic strengthening of the remaining inputs, however, appear to differ between the NMJ and the retinogeniculate synapse. At the NMJ, there is a transition from synaptic facilitation in young animals to depression in old animals, consistent with a marked enhancement in the probability of release (Bennett and Pettigrew, 1974). In contrast, we find that over the developmental time of our study there is not a significant change in the release probability at the retinogeniculate synapse. In addition, while we observe a significant enhancement in the quantal size for the strengthened retinogeniculate input, similar increases have not been observed at the mammalian NMJ (Diamond and Miledi, 1962). Finally, we find an enhancement in the number of release sites of the remaining retinal inputs. At the NMJ, the quantal content increases (Colman et al., 1997), however, the relative contribution of release probability and number of release sites to this change is unclear.

Thus it appears that many features of synaptic refinement are tailored to specific synapses. It will be interesting to see if the mechanisms important in the remodeling of the retinogeniculate synapses are also involved in the refinement of other connections of the central nervous system.

Experimental Procedures

DiI Injections

The neuronal label DiI (Molecular Probes, Oregon, 20%–30% w/vol) was injected into the 4 quadrants of the retina of anesthesized Black Swiss mice ranging from postnatal day 10–31. The animal was allowed to recover from halothane anesthesia (Halocarbon) and kept alive for 1–2 days to permit diffusion of the dye to the lateral geniculate body after which they were sacrificed and brain slices were cut. DiI injections were used to visualize the retinogeniculate connections during the optimization of the dLGN slice configuration. There were no obvious effects of DiI labeling on synaptic transmission at the retinogeniculate synapse. Nonetheless, all of the electrophysiology data shown in this paper were obtained from unlabeled animals.

LGN Slice Preparation

Parasagittal brain slices containing the dorsal lateral geniculate nucleus (dLGN) were obtained from p10–31 Black Swiss mice using a modified protocol described by Turner and Salt (Turner and Salt,

1998). Briefly, the brain was removed rapidly and immersed into an oxygenated 4°C saline solution containing (in mM): 125 NaCl, 2.5 KCl, 2.6 $NaHCO_3$, 1.25 NaH_2PO_4, 25 glucose, 2 $CaCl_2$, and 1 $MgCl_2$.

The two hemispheres were first separated by an angled cut (10°–20°) relative to the cerebral longitudinal fissure. The medial aspect of the brain was then glued onto a tilted (15°–25°) cutting stage of a vibratome (Leica VT1000S). The tissue section was submerged into an oxygenated 1°–4°C saline solution and 250–300 μm sections were cut with a sapphire blade (DDK). In general, only a single slice from a given hemisphere contained the optic tract and its fibers radiating to the dLGN. Slices were allowed to recover over 1 hr in oxygenated saline at 30°C before electrophysiological recordings.

Electrophysiology

Whole-cell voltage clamp recordings of geniculate neurons were obtained under visual guidance (Zeiss Axioskop, 60X immersion objective, NA 0.9) using 1.2–2.0 M patch electrodes containing the internal solution (in mM): 35 CsF, 100 CsCl, 10 EGTA, 10 HEPES, 0.1 D600 (pH 7.4). Leak currents at −70 mV with this solution ranged from −50 to −110 pA, −50 to −280 pA and −85 to −230 pA for p10–14, p16–22 and p23–31 mice, respectively. Geniculate neurons were distinguished from the local inhibitory neurons by their larger size (15–25 μm in diameter), and by the number of dendrites coming off of the cell body (three or more dendrites). In contrast, inhibitory neurons are smaller (<12 μm in diameter) and have bipolar morphology. Cells located in the proximal 2/3 of the dLGN relative to the optic tract (lateral and caudal aspects of the dLGN) were preferentially recorded from since they were more likely to have intact connections with the optic tract. Slices were continuously perfused with a bubbled 95%O_2/5% CO_2 extracellular saline solution at 24°C. To prevent excitatory disynaptic connections (the recurrent loop between geniculate and corticothalamic neurons), the cortex was separated from the thalamus with a razor incision through the white matter tracts. Inhibitory disynaptic connections (between intrinsic inhibitory neurons as well as neurons from the nucleus reticularis) were eliminated by recording in a solution containing the $GABA_A$ antagonist, 20 μM bicuculline. A pair of glass filled saline electrodes (12–25 μm tip diameter) were used to stimulate the optic tract with intensities ranged from 1–40 μA (duration 0.2 ms). Repetitive stimulations (0.025–0.05 Hz) at intensities greater than 40 μA resulted in a decrement in the synaptic response, most likely due to loss of axon fibers. The membrane potential of the geniculate neurons was clamped at either −70 mV or +40 mV during stimulation of the optic tract, and at 0 mV between stimulation trials. Quantal events at retinogeniculate synapses were resolved in the presence of an oxygenated extracellular solution containing (in mM): 3 Sr Cl_2, 2 Mg Cl_2, 125 NaCl, 2.5 KCl, 2.6 $NaHCO_3$, 1.25 NaH_2PO_4, 25 glucose and 20 μM bicuculline. Stock solutions of NMDAR and non-NMDAR antagonists, D(-)-AP5 (2-Amino-5-phosphonopentanoic acid), CPP (3-(R)-2-carboxypiperazin-4-yl)-propyl-1-phosphonic acid, 5 mM) and NBQX (2,3-dioxo-6-nitro-1,2,3,4-tetrahydrobenzo[f]quinoxaline-7-sulfonamide disodium, 10 mM) respectively, (Tocris, MO) were stored in dH_2O at −20°C and diluted to the final concentration just before addition to the bath solution.

Single Fiber Recordings

The amplitude of the synaptic current from minimal stimulation was taken to be the single fiber response. In cases where it was not possible to obtain such clear-cut activation of single fibers the stimulus electrode was repositioned and the procedure resumed. Since trial-to-trial variability in the amplitude of the synaptic current was relatively small (see Figure 4B,C), most values were obtained from single trials. For small inputs (<10 pA), multiple trials were obtained and the average amplitude was used. In the case of silent fibers, six to ten consecutive trials (alternately testing for a NMDAR and AMPAR component at a constant stimulus intensity) were obtained to assure that failures were reproducible at −70 mV. In some experiments, a second input was clearly resolvable from the first. These inputs were also included in the amplitude histogram. In general, the threshold response for the NMDAR and AMPAR component occurred at the same stimulus intensity except in young animals, p10–14, where silent fibers were found. The stimulus intensities required to elicit a single fiber threshold response does not change significantly over this developmental period (in μA: p10–14, 13 ± 1, n = 31; p16–22, 17 ± 1, n = 48; p23–31, 16 ± 3, n = 30).

Probability of Release

A widely used method of monitoring release probability is to study the rate of blockade of the NMDAR EPSC by the open channel blocker, MK-801 (Hessler et al., 1993; Rosenmund et al., 1993). Unfortunately, the subunit changes in the NMDAR at retinogeniculate synapses during this developmental time window are associated with changes in the gating kinetics and sensitivity of NMDAR inhibitors, make interpretation of MK-801 experiments difficult (Monyer et al., 1994; Monyer et al., 1992; Ramoa and Prusky, 1997).

Therefore, rather than using MK-801, we monitored the paired-pulse ratio. AMPAR EPSCs elicited by pairs of stimuli, separated by 100 ms, were interleaved with EPSCs elicited by a single stimulus. The average of 3–5 trials was used to calculate the ppr (100*A2/A1) of a given cell. A1 is the average peak EPSCs in response to a single stimulation. The amplitude of the second EPSC, A2, is measured from the waveform obtained by subtracting the average single EPSC response from the average EPSC response to a pair of stimuli. We compared ppr over a range of ages in the presence of 20 μM CTZ and at a holding potential of +40 mV. At this holding potential, 20 μM CTZ does not have presynaptic effects at the retinogeniculate synapse (Figure 7b). An increase in CTZ to 50 μM did not further alter ppr of the AMPAR component when compared to 20 μM CTZ.

Data Acquisition and Analysis

Optic tract evoked EPSCs were obtained with the Axopatch 200B (Axon Instruments). In all experiments except those involving extracellular strontium, the currents were sampled at 10–20 kHz with an ITC-16 interface (Instrutech) and filtered at 1 kHz. Stimulus-evoked currents from experiments that resolved quantal events were filtered at 5 kHz with a 4-pole Bessel filter and digitized at 20 kHz. Quantal events were detected and analyzed off-line using IGOR PRO software (Wavemetrics, Lake Osowego, OR) and custom macros. Events larger than 3.5 pA were detected based on the threshold crossing of the first derivative (5 $pAms^{-1}$, following 500 Hz, 4-pole digital filtering). Identical detection procedures and parameters were use for all experiments.

Acknowledgments

We thank K. Vogt, M. Xu-Friedman, A. Carter, A. Kreitzer, K. Foster, R.C. Reid, S. Tavazoie, and C.J. Shatz for advice and comments on the manuscript. This work was supported by NIH R01-NS32405 and P01-NS38312 to W.R. and NIH K08-NS02056 to C.C.

Received July 31, 2000; revised October 26, 2000.

References

Aiba, A., Kano, M., Chen, C., Stanton, M.E., Fox, G.D., Herrup, K., Zwingman, T.A., and Tonegawa, S. (1994). Deficient cerebellar long-term depression and impaired motor learning in mGluR1 mutant mice. Cell *79*, 377–388.

Artola, A., Brocher, S., and Singer, W. (1990). Different voltage-dependent thresholds for inducing long-term depression and long-term potentiation in slices of rat visual cortex. Nature *347*, 69–72.

Bellingham, M.C., Lim, R., and Walmsley, B. (1998). Developmental changes in EPSC quantal size and quantal content at a central glutamatergic synapse in rat. J. Physiol. *511*, 861–869.

Bellingham, M.C., and Walmsley, B. (1999). A novel presynaptic inhibitory mechanism underlies paired pulse depression at a fast central synapse. Neuron *23*, 159–170.

Bennett, M.R., and Pettigrew, A.G. (1974). The formation of synapses in striated muscle during development. J. Physiol. *241*, 515–545.

Bi, G., and Poo, M. (1999). Distributed synaptic modification in neural networks induced by patterned stimulation. Nature *401*, 792–796.

Blakemore, C., Garey, L.J., and Vital-Durand, F. (1978). The physiological effects of monocular deprivation and their reversal in the monkey's visual cortex. J. Physiol. *283*, 223–262.

Blakemore, C., and Vital-Durand, F. (1986). Organization and post-

natal development of the monkey's lateral geniculate nucleus. J. Physiol. *380*, 453–491.

Brown, M.C., Jansen, J.K., and Van Essen, D. (1976). Polyneuronal innervation of skeletal muscle in new-born rats and its elimination during maturation. J. Physiol. *261*, 387–422.

Campbell, G., and Shatz, C.J. (1992). Synapses formed by identified retinogeniculate axons during the segregation of eye input. J. Neurosci. *12*, 1847–1858.

Carmignoto, G., and Vicini, S. (1992). Activity-dependent decrease in NMDA receptor responses during development of the visual cortex. Science *258*, 1007–1011.

Chuhma, N., and Ohmori, H. (1998). Postnatal development of phase-locked high-fidelity synaptic transmission in the medial nucleus of the trapezoid body of the rat. Journal of Neuroscience *18*, 512–520.

Cleland, B.G., Dubin, M.W., and Levick, W.R. (1971). Simultaneous recording of input and output of lateral geniculate neurones. Nature - New Biology *231*, 191–192.

Colman, H., Nabekura, J., and Lichtman, J.W. (1997). Alterations in synaptic strength preceding axon withdrawal. Science *275*, 356–361.

Constantine-Paton, M., and Cline, H.T. (1998). LTP and activity-dependent synaptogenesis: the more alike they are, the more different they become. Curr. Opin. Neurobiol. *8*, 139–148.

Constantine-Paton, M., Cline, H.T., and Debski, E. (1990). Patterned activity, synaptic convergence, and the NMDA receptor in developing visual pathways. Annu. Rev. Neurosci. *13*, 129–154.

Crepel, F., Mariani, J., and Delhaye-Bouchaud, N. (1976). Evidence for a multiple innervation of Purkinje cells by climbing fibers in the immature rat cerebellum. J. Neurobiol. *7*, 567–578.

Daniels, J.D., Pettigrew, J.D., and Norman, J.L. (1978). Development of single-neuron responses in kitten's lateral geniculate nucleus. J. Neurophysiol. *41*, 1373–1393.

Davis, G.W., and Goodman, C.S. (1998). Synapse-specific control of synaptic efficacy at the terminals of a single neuron. Nature *392*, 82–86.

Diamond, J., and Miledi, R. (1962). A study of foetal and new-born rat muscle fibres. J. Physiol. *162*, 393–408.

Diamond, J.S., and Jahr, C.E. (1995). Asynchronous release of synaptic vesicles determines the time course of the AMPA receptor-mediated EPSC. Neuron *15*, 1097–1107.

Dittman, J.S., and Regehr, W.G. (1998). Calcium dependence and recovery kinetics of presynaptic depression at the climbing fiber to Purkinje cell synapse. J. Neurosci. *18*, 6147–6162.

Durand, G.M., Kovalchuk, Y., and Konnerth, A. (1996). Long-term potentiation and functional synapse induction in developing hippocampus. Nature *381*, 71–75.

Fagiolini, M., Pizzorusso, T., Berardi, N., Domenici, L., and Maffei, L. (1994). Functional postnatal development of the rat primary visual cortex and the role of visual experience: dark rearing and monocular deprivation. Vision Res. *34*, 709–720.

Fraser, S.E. (1992). Patterning of retinotectal connections in the vertebrate visual system. Curr. Opin. Neurobiol. *2*, 83–87.

Freeman, R.D., and Olson, C. (1982). Brief periods of monocular deprivation in kittens: effects of delay prior to physiological study. J. Neurophysiol. *47*, 139–150.

Goda, Y., and Stevens, C.F. (1994). Two components of transmitter release at a central synapse. Proc. Natl. Acad. Sci. USA *91*, 12942–12946.

Godement, P., Salaun, J., and Imbert, M. (1984). Prenatal and postnatal development of retinogeniculate and retinocollicular projections in the mouse. J. Comp. Neurol. *230*, 552–575.

Golshani, P., and Jones, E.G. (1999). Synchronized paroxysmal activity in the developing thalamocortical network mediated by corticothalamic projections and "silent" synapses. J. Neurosci. *19*, 2865–2875.

Golshani, P., Warren, R.A., and Jones, E.G. (1998). Progression of change in NMDA, non-NMDA, and metabotropic glutamate receptor function at the developing corticothalamic synapse. J. Neurophysiol. *80*, 143–154.

Gordon, J.A., and Stryker, M.P. (1996). Experience-dependent plasticity of binocular responses in the primary visual cortex of the mouse. J. Neurosci. *16*, 3274–3286.

Hamori, J., Pasik, P., and Pasik, T. (1991). Different types of synaptic triads in the monkey dorsal lateral geniculate nucleus. Journal fur Hirnforschung *32*, 369–379.

Hamos, J.E., Van Horn, S.C., Raczkowski, D., and Sherman, S.M. (1987). Synaptic circuits involving an individual retinogeniculate axon in the cat. J. Comp. Neurol. *259*, 165–192.

Hamos, J.E., Van Horn, S.C., Raczkowski, D., Uhlrich, D.J., and Sherman, S.M. (1985). Synaptic connectivity of a local circuit neurone in lateral geniculate nucleus of the cat. Nature *317*, 618–621.

Hensch, T.K., Fagiolini, M., Mataga, N., Stryker, M.P., Baekkeskov, S., and Kash, S.F. (1998). Local GABA circuit control of experience-dependent plasticity in developing visual cortex. Science *282*, 1504–1508.

Hessler, N.A., Shirke, A.M., and Malinow, R. (1993). The probability of transmitter release at a mammalian central synapse. Nature *366*, 569–572.

Hestrin, S. (1992). Developmental regulation of NMDA receptor-mediated synaptic currents at a central synapse. Nature *357*, 686–689.

Hohnke, C.D., and Sur, M. (1999). Stable properties of spontaneous EPSCs and miniature retinal EPSCs during the development of ON/OFF sublamination in the ferret lateral geniculate nucleus. J. Neurosci. *19*, 236–247.

Hubel, D.H., Wiesel, T.N., and LeVay, S. (1977). Plasticity of ocular dominance columns in monkey striate cortex. Philos. Trans. R. Soc. Lond. B. Biol. Sci. - Series B. Biol. Sci. *278*, 377–409.

Isaac, J.T., Nicoll, R.A., and Malenka, R.C. (1995). Evidence for silent synapses: implications for the expression of LTP. Neuron *15*, 427–434.

Isaac, J.T.R., Crair, M.C., Nicoll, R.A., and Malenka, R.C. (1997). Silent synapses during development of thalamocortial inputs. Neuron *18*, 269–280.

Jackson, H., and Parks, T.N. (1982). Functional synapse elimination in the developing avian cochlear nucleus with simultaneous reduction in cochlear nerve axon branching. J. Neurosci. *2*, 1736–1743.

Kano, M., Hashimoto, K., Chen, C., Abeliovich, A., Aiba, A., Kurihara, H., Watanabe, M., Inoue, Y., and Tonegawa, S. (1995). Impaired synapse elimination during cerebellar development in PKC gamma mutant mice. Cell *83*, 1223–1231.

Kato, N., Artola, A., and Singer, W. (1991). Developmental changes in the susceptibility to long-term potentiation of neurones in rat visual cortex slices. Brain Res. Dev. Brain Res. *60*, 43–50.

Katz, L.C., and Shatz, C.J. (1996). Synaptic activity and the construction of cortical circuits. Science *274*, 1133–1138.

Kirkwood, A., Dudek, S.M., Gold, J.T., Aizenman, C.D., and Bear, M.F. (1993). Common forms of synaptic plasticity in the hippocampus and neocortex in vitro. Science *260*, 1518–1521.

Kirkwood, A., Lee, H.K., and Bear, M.F. (1995). Co-regulation of long-term potentiation and experience-dependent synaptic plasticity in visual cortex by age and experience. Nature *375*, 328–331.

Kutsuwada, T., Kashiwabuchi, N., Mori, H., Sakimura, K., Kushiya, E., Araki, K., Meguro, H., Masaki, H., Kumanishi, T., and Arakawa, M. (1992). Molecular diversity of the NMDA receptor channel. Nature *358*, 36–41.

LeVay, S., Wiesel, T.N., and Hubel, D.H. (1980). The development of ocular dominance columns in normal and visually deprived monkeys. J. Comp. Neurol. *191*, 1–51.

Lichtman, J.W. (1977). The reorganization of synaptic connexions in the rat submandibular ganglion during post-natal development. J. Physiol. *273*, 155–177.

Lichtman, J.W., and Colman, H. (2000). Synapse elimination and indelible memory. Neuron *25*, 269–278.

Linden, D.C., Guillery, R.W., and Cucchiaro, J. (1981). The dorsal

lateral geniculate nucleus of the normal ferret and its postnatal development. J. Comp. Neurol. *203*, 189–211.

Luscher, C., Xia, H., Beattie, E.C., Carroll, R.C., von Zastrow, M., Malenka, R.C., and Nicoll, R.A. (1999). Role of AMPA receptor cycling in synaptic transmission and plasticity. Neuron *24*, 649–658.

Malenka, R.C., and Nicoll, R.A. (1999). Long-term potentiation—a decade of progress? Science *285*, 1870–1874.

Mariani, J., and Changeux, J.P. (1981). Ontogenesis of olivocerebellar relationships. I. Studies by intracellular recordings of the multiple innervation of Purkinje cells by climbing fibers in the developing rat cerebellum. J. Neurosci. *1*, 696–702.

Mason, C.A. (1982). Development of terminal arbors of retino-geniculate axons in the kitten—I. Light microscopical observations. Neuroscience *7*, 541–559.

Mastronarde, D.N. (1992). Nonlagged relay cells and interneurons in the cat lateral geniculate nucleus: receptive-field properties and retinal inputs. Vis. Neurosci. *8*, 407–441.

Miledi, R. (1966). Strontium as a substitute for calcium in the process of transmitter release at the neuromuscular junction. Nature *212*, 1233–1234.

Monyer, H., Burnashev, N., Laurie, D.J., Sakmann, B., and Seeburg, P.H. (1994). Developmental and regional expression in the rat brain and functional properties of four NMDA receptors. Neuron *12*, 529–540.

Monyer, H., Sprengel, R., Schoepfer, R., Herb, A., Higuchi, M., Lomeli, H., Burnashev, N., Sakmann, B., and Seeburg, P.H. (1992). Heteromeric NMDA receptors: molecular and functional distinction of subtypes. Science *256*, 1217–1221.

Mooney, R., Madison, D.V., and Shatz, C.J. (1993). Enhancement of transmission at the developing retinogeniculate synapse. Neuron *10*, 815–825.

O'Brien, R.A., Ostberg, A.J., and Vrbova, G. (1978). Observations on the elimination of polyneuronal innervation in developing mammalian skeletal muscle. J. Physiol. *282*, 571–582.

O'Brien, R.J., Kamboj, S., Ehlers, M.D., Rosen, K.R., Fischbach, G.D., and Huganir, R.L. (1998). Activity-dependent modulation of synaptic AMPA receptor accumulation. Neuron *21*, 1067–1078.

Purves, D., and Lichtman, J.W. (1980). Elimination of synapses in the developing nervous system. Science *210*, 153–157.

Rafols, J.A., and Valverde, F. (1973). The structure of the dorsal lateral geniculate nucleus in the mouse. A Golgi and electron microscopic study. J. Comp. Neurol. *150*, 303–332.

Ramoa, A.S., and McCormick, D.A. (1994). Enhanced activation of NMDA receptor responses at the immature retinogeniculate synapse. J. Neurosci. *14*, 2098–2105.

Ramoa, A.S., and Prusky, G. (1997). Retinal activity regulates developmental switches in functional properties and ifenprodil sensitivity of NMDA receptors in the lateral geniculate nucleus. Brain Res. Dev. Brain Res. *101*, 165–175.

Rosenmund, C., Clements, J.D., and Westbrook, G.L. (1993). Nonuniform probability of glutamate release at a hippocampal synapse. Science *262*, 754–757.

Rumpel, S., Hatt, H., and Gottmann, K. (1998). Silent synapses in the developing rat visual cortex: evidence for postsynaptic expression of synaptic plasticity. J. Neurosci. *18*, 8863–8874.

Shatz, C.J., and Kirkwood, P.A. (1984). Prenatal development of functional connections in the cat's retinogeniculate pathway. J. Neurosci. *4*, 1378–1397.

Shatz, C.J., and Stryker, M.P. (1978). Ocular dominance in layer IV of the cat's visual cortex and the effects of monocular deprivation. J. Physiol. *281*, 267–283.

Shi, J., Aamodt, S.M., and Constantine-Paton, M. (1997). Temporal correlations between functional and molecular changes in NMDA receptors and GABA neurotransmission in the superior colliculus. J. Neurosci. *17*, 6264–6276.

Shi, S.H., Hayashi, Y., Petralia, R.S., Zaman, S.H., Wenthold, R.J., Svoboda, K., and Malinow, R. (1999). Rapid spine delivery and redistribution of AMPA receptors after synaptic NMDA receptor activation. Science *284*, 1811–1816.

Sretavan, D.W., and Shatz, C.J. (1986). Prenatal development of retinal ganglion cell axons: segregation into eye-specific layers within the cat's lateral geniculate nucleus. J. Neurosci. *6*, 234–251.

Sur, M., Weller, R.E., and Sherman, S.M. (1984). Development of X- and Y-cell retinogeniculate terminations in kittens. Nature *310*, 246–249.

Tavazoie, S.F., and Reid, R.C. (2000). Diverse receptive fields in the lateral geniculate nucleus during thlamocortical development. Nat. Neurosci. *3*, 608–616.

Tootle, J.S., and Friedlander, M.J. (1989). Postnatal development of the spatial contrast sensitivity of X- and Y-cells in the kitten retinogeniculate pathway. J. Neurosci. *9*, 1325–1340.

Trachtenberg, J.T., Trepel, C., and Stryker, M.P. (2000). Rapid extragranular plasticity in the absence of thalamocortical plasticity in the developing primary visual cortex. Science *287*, 2029–2032.

Turner, J.P., and Salt, T.E. (1998). Characterization of sensory and corticothalamic excitatory inputs to rat thalamocortical neurones in vitro. J. Physiol. *510*, 829–843.

Usrey, W.M., Reppas, J.B., and Reid, R.C. (1999). Specificity and strength of retinogeniculate connections. J. Neurophysiol. *82*, 3527–3540.

Watt, A.J., van Rossum, M.C., MacLeod, K.M., Nelson, S.B., and Turrigiano, G.G. (2000). Activity coregulates quantal AMPA and NMDA currents at neocortical synapses. Neuron *26*, 659–670.

Wu, G., Malinow, R., and Cline, H.T. (1996). Maturation of a central glutamatergic synapse. Science *274*, 972–976.

Xu-Friedman, M.A., and Regehr, W.G. (1999). Presynaptic strontium dynamics and synaptic transmission. Biophys. J. *76*, 2029–2042.